



1180 nm GaInNAs quantum well based high power DBR laser diodes

Citation

Vihariälä, J., Aho, A., Virtanen, H., Koskinen, M., Dumitrescu, M., & Guina, M. (2017). 1180 nm GaInNAs quantum well based high power DBR laser diodes. In M. S. Zediker (Ed.), *High-Power Diode Laser Technology XV* [100860K] (Proceedings of SPIE; Vol. 10086). SPIE. <https://doi.org/10.1117/12.2251317>

Year

2017

Version

Peer reviewed version (post-print)

Link to publication

[TUTCRIS Portal \(http://www.tut.fi/tutcris\)](http://www.tut.fi/tutcris)

Published in

High-Power Diode Laser Technology XV

DOI

[10.1117/12.2251317](https://doi.org/10.1117/12.2251317)

Copyright

This publication is copyrighted. You may download, display and print it for Your own personal use. Commercial use is prohibited.

Take down policy

If you believe that this document breaches copyright, please contact cris.tau@tuni.fi, and we will remove access to the work immediately and investigate your claim.

1180 nm GaInNAs quantum well based high power DBR laser diodes

Jukka Viheriälä, Antti T. Aho., Heikki Virtanen, Mervi Koskinen, Michael Dumitrescu
and Mircea Guina

Optoelectronics Research Centre, Tampere University of Technology, Tampere, Finland

ABSTRACT

We summarize the recent development in narrow spectrum 1180 nm (narrow linewidth) laser diodes based on GaInNAs quantum wells and show results for ridge waveguide DBR laser diode including its reliability tests. Manuscript demonstrates 500 mW output power in continuous-wave operation at room temperature, wide single mode tuning region and narrow linewidth operation. Devices reached narrow linewidth operation (<250 kHz) across their operation band.

Keywords: GaInNAs quantum well, DBR laser diode, tapered laser diode, Second harmonic generation, distributed bragg reflector, Nanoimprint lithography

1. INTRODUCTION

We summarize the recent development in narrow spectrum 1180 nm GaInNAs-Quantum Well based distributed Bragg reflector (DBR) laser diodes with CW output power up to 500 mW from Ridge Waveguide (RWG)-DBR laser diodes. The work presented here is aimed for applications in second harmonic generation (SHG). RWG-DBR LDs are optimal light sources for waveguide SHG-crystals where the high efficiency coupling is required from laser diode to single mode WG embedded in the SHG-crystal. High performance results shown here are enabled by the use of novel Nitrogen alloyed GaInNAs quantum wells embedded in GaAs Waveguide. The preliminary lifetime test for RWG-DBR LDs showed no degradation in a room-temperature lifetime test with 1500 mA drive-current for over 2000 hours. These compact and efficient 1180 nm laser diodes are instrumental for the development of compact frequency doubled yellow–orange lasers, which have important applications in spectroscopy and medicine, such as the treatment of vascular lesions. These would benefit from the availability of compact semiconductor lasers emitting at yellow–orange wavelengths. However, this wavelength range cannot be reached with compact and efficient directly emitting semiconductor lasers typically employed for red wavelengths (GaAs-based compounds) or for blue–green wavelengths (GaN-based materials). Moreover, the frequency doubling approaches, traditionally used for reaching the green wavelength range, suffer from the lack of high-power narrow-linewidth frequency-stable laser diodes emitting at 1170–1250 nm. This is due to the fact that GaInAs/GaAs QWs for this wavelength range require a high In content, leading to high strain that generate a high amount of defects, which affect the laser efficiency and life-time.

The 1180 nm wavelength range can be reached using dilute nitrides, i.e. GaInNAs/GaAs QWs. The use of a small amount of N, in the range of 1 %, has been recognized for its benefits related to reduced strain and good carrier confinement, enabling power levels beyond 10 W in optically pumped vertical-external-cavity surface-emitting lasers (VECSELs) [1]. The improved carrier confinement translates to improved temperature stability of the laser characteristics, a feature that has been recognized since the proposal of GaInNAs/GaAs QWs for uncooled telecom lasers at 1.3 μm [2]. The improved temperature stability is expected to benefit especially the miniaturization of frequency-doubled lasers and in general the development of photonic integration approaches, which are currently limited by thermal management issues. For example, the ability of lasers to operate at elevated temperatures will reduce the constraints of mounting them close to frequency doubling crystals, which often require elevated operation temperatures [3].

*Jukka.Viheriala@tut.fi; phone +358 50 595 4147; www.orc.tut.fi

Research was supported by EU funding using projects FP7-SEM, APACOS (Grant agreement ID: 315711) and ECSEL DENSE (Grant agreement ID: 692449)

2. GROWTH OF LASER DIODE WAFER

Symmetric large optical cavity structure was grown by plasma-assisted molecular beam epitaxy (MBE) on an n-GaAs(100) substrate and consisted of a single GaIn_{0.31}N_{0.005}As QW embedded in a 1 μm GaAs waveguide surrounded by Al_{0.25}GaAs claddings. The QW was grown at low temperature of 380 $^{\circ}\text{C}$ in order to kinetically limit phase separation of metastable GaInNAs [4, 5]. We used an excess arsenic pressure corresponding to a beam equivalent pressure ratio of As/III = 14. A high growth rate of 1.4 $\mu\text{m}/\text{h}$ was chosen to keep the nitrogen composition low [6]. On the p-side, thinner cladding was used for alleviating possible problems due to high aspect ratio etching of the DBR and to maximize thermal conductivity towards p-contact.

In addition to precisely controlled growth conditions, post-growth annealing is of high-importance in GaInNAs device fabrication. Annealing reduces the amount of point defects related to low-temperature growth and nitrogen incorporation and affects nitrogen-induced short range ordering. This improves the luminescence intensity but also induces a blue shift of the emission wavelength. However, the unwanted blue shift is saturable and thus, easily controlled assuming that annealing temperature is not increased above 750 $^{\circ}\text{C}$ [4, 7]. In order to improve material quality for the lasers reported here, we grew three test structures with different annealing temperatures: ~ 695 , ~ 705 and ~ 720 $^{\circ}\text{C}$. As a result of increased annealing temperature, photoluminescence (PL) intensity of the laser wafers increased by an order of magnitude, and threshold current density of broad area test lasers decreased to one third of the original value. The best wafer showed PL wavelength of 1173 nm and lasing wavelengths above 1190 nm, which are too high for the targeted 1180 nm DBR laser wavelength. For the DBR laser, we chose an annealing temperature of ~ 720 $^{\circ}\text{C}$, fine-tuned the QW emission wavelength by slightly reducing In and N compositions. Table 1 lists the key characteristics obtained from broad area laser diodes.

The determined characteristics temperatures were $T_0 = 110$ K and $T_1 = 160$ K. For comparison, typical T_0 values for InGaAs/GaAs QWs with similar wavelength are around 80 K [8, 9]. In fact we measured a $T_0 = 80$ K and $T_1 = 130$ K for our InGaAs/GaAs laser with similar structure but emitting at 1060 nm. Still, it should be noted that regardless of the QW material these values can be improved using higher number of QWs or AlGaAs barriers. Increasing the number of QWs using dilute nitrides should be easier than with GaInAs because of the smaller lattice mismatch. Wavelength of the broad-area lasers shifted at a rate of 0.41 nm/ $^{\circ}\text{C}$ and was centered at 1180 nm at a mount temperature of 100 $^{\circ}\text{C}$. The vertical far field had a full width at half maximum of 43 $^{\circ}$.

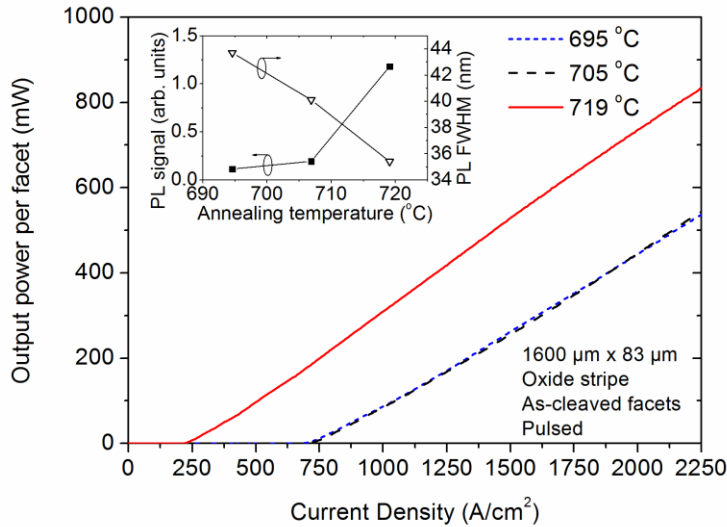


Figure 1. Pulsed output power characteristics of 1180 nm broad area laser diodes prepared with different kind of QW annealing conditions. Results are from as-cleaved devices.

Table 1. Operating characteristics for 1180 nm GaInNAs QW material and laser structure

Parameter	Value
Wavelength shift vs temperature	0.41 nm / K
T ₀	110 K
T ₁	160 K
Fast axis Far Field divergence	43deg FWHM

3. DEVICE FABRICATION

The DBR laser structure comprises a 3 mm long straight ridge waveguide (RWG) gain section and a 2 mm long passive/unbiased DBR section. The RWG section was designed to provide the maximum modal area for the fundamental mode while also to act as a transverse mode filter, preventing higher-order transverse modes in the laser cavity. TE mode emission is ensured by the compressive QW strain and by better surface grating reflectivity for the TE mode. The optimization of the RWG dimensions was achieved by simulation and experimental studies of the gain and index guiding properties of the structure. A 3.2 μ m ridge width and a 1.4 μ m etching depth was chosen based on experimental far-field pattern and LIV characteristic optimization studies, which suggested that these dimensions would provide the best combination of transverse mode filtering, relatively low threshold current, and high efficiency. A 3 mm long straight RWG gain section was employed to achieve a high output power.

The laser cavity has cleaved and anti-reflection (AR) coated end facets. A 3-rd order DBR surface grating with 50% filling-factor trapezoidal-shaped teeth was formed as shown in Figure 2 To ensure high wavelength selectivity, the DBR mirror was designed to have a relatively narrow stopband, spectrally aligned with the gain peak of the RWG active region. Because of the narrow stopband of the DBR mirror, the resonant cavity supports only the longitudinal mode that is closest to the gain peak and has the lowest mirror losses, generating a stable single-longitudinal mode emission.

The surface grating was fabricated using soft stamp ultraviolet nanoimprint lithography (UV-NIL) using process described in reference [10]. The soft UV-NIL stamp comprised a thin layer of patterned hard polydimethylsiloxane (PDMS) on a thin glass substrate (employed to avoid lateral deformation during imprinting), superimposed with a soft PDMS cushion and a thick glass plate. After the epitaxial growth, the epiwafer was coated with a 300 nm thick layer of SiO₂, polydimethylglutarimide (PMGI) and mr-UVcur06 (Microresist Technology GmbH) UV-NIL resist, before imprinting the etch mask profiles onto the NIL-resist by the soft UV-NIL-stamp. Subsequently, the residual resist layer was removed with oxygen plasma by reactive ion etching (RIE), and the PMGI was developed. The underlying SiO₂ layer was exposed on imprinted areas and a small undercut to the PMGI profile was left behind. After a 10 nm thick layer of nickel was deposited on the patterned epiwafer by electron-beam evaporation, the remaining PMGI was removed with a solvent. The nickel on top of it was lifted off and the metal etch mask was left on the SiO₂ layer.

The device surface structures were etched onto the epiwafer by etching first through the SiO₂ layer using RIE with the ridge and the grating regions protected by the nickel mask. The semiconductor layers were etched by Cl₂/N₂ and by inductively coupled plasma (ICP). Because the ridge and the grating structure had different etching rates (i.e. higher etch rate for the RWG) and slightly different target etching depths (1420 nm for the RWG section and 1440 nm for the DBR section), the RWG section was protected with a photoresist after it reached the target etching depth and the etching was continued for the grating section to obtain the required etching depth and the designed grating reflectivity. After the protective photoresist was removed, the structure was planarized with benzocyclobutene (BCB) and a 230 nm thick layer of SiO₂ was deposited on the patterned wafer. The contact region was patterned by UV-photolithography and opened using RIE. Ti/Pt/Au was deposited as the p-contact. The wafer was then thinned down to about 130 μ m. The n-contact was then formed by a stack of Ni/Au/Ge/Au, followed by rapid thermal annealing under N₂ ambient at 370 °C for 60 s. Finally the wafer was diced and a Al₂O₃ / TiO₂ AR coating was deposited on the end facets, resulting in a reflectivity below 1% at 1180 nm.

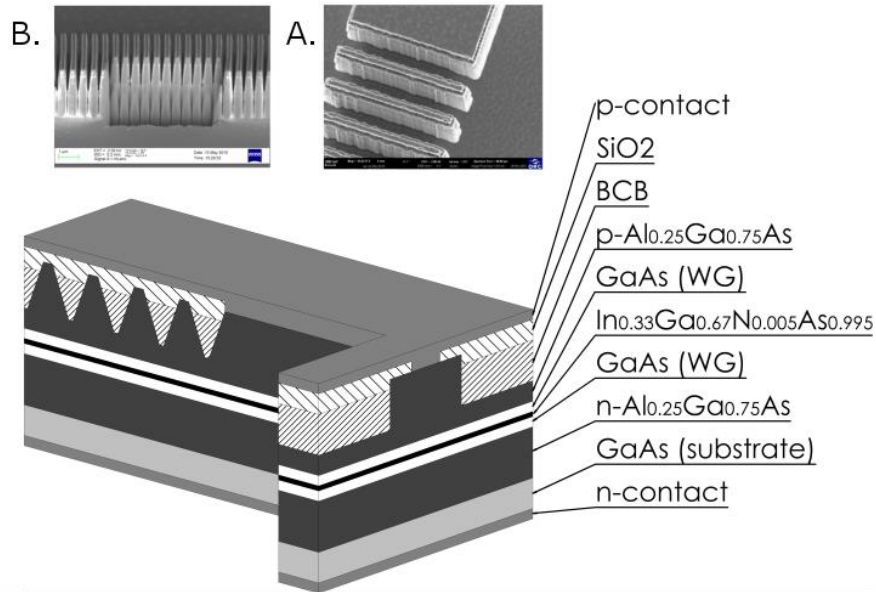


Figure 2. The device layout. SEM micrographs A and B show detail from the grating directly after the dry etching step used to prepare them.

4. RESULTS

LIV-characteristics

The lasers were first mounted p-side down on AlN-submounts, and then onto copper heat sinks with indium solder to provide efficient heat dissipation. The LIV-characteristics of the devices were measured in continuous wave operation with a thermoelectric cooler that maintained a constant 20 °C. The temperature was measured by a temperature transducer AD590 from the bottom of the heat sink. The LIV-measurements shown in Figure 3 reveal a state-of-the-art continuous wave (CW) output power of 500 mW in single-mode operation for a current of 1630 mA. At high drive currents (above 1630 mA) the lasing mode starts to hop from one longitudinal mode to another and the output power saturates. The light-current (LI) curve has no kinks or mode-hop jumps from threshold almost up to roll-over.

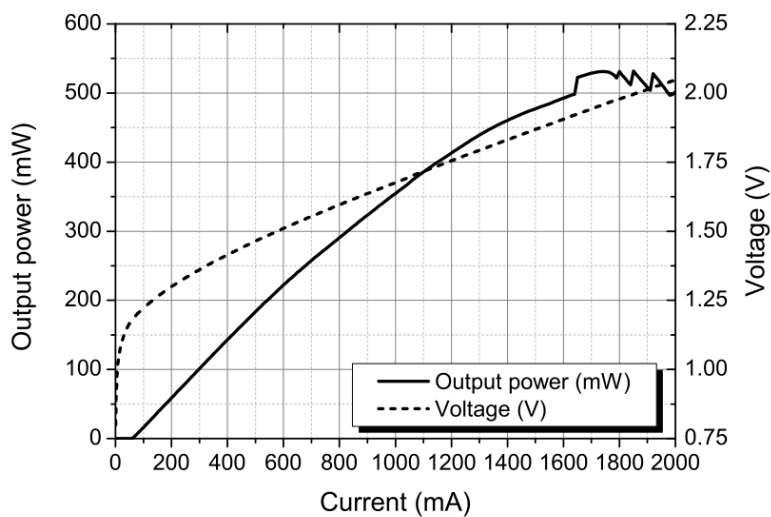


Figure 3. LIV characteristics of the DBR-LDs

4.2 Linewidth measurements

The emission linewidth has been measured by a self-homodyne measurement system [11]. The self-homodyne method relies on the double-arm interferometer where the laser light is mixed with a delayed replica of itself and the interference signal is fed into a photodiode that generates the autocorrelation function. The Fourier transform of the autocorrelation function returns a lineshape with a spectral full-width-at-half-maximum (FWHM) that is two times the spectral FWHM of the emitted laser lineshape [12].

This is valid only if the mixed laser spectra are uncorrelated; therefore the delay line must be longer than the coherence length of the laser light. Hence, a 2 km long fiber delay line, longer than the coherence length corresponding to a 100 kHz Lorentzian lineshape linewidth, was used to ensure that the optical signals on both arms of the interferometer were uncorrelated. Moreover, the photodiode was unbiased in order to reduce the noise.

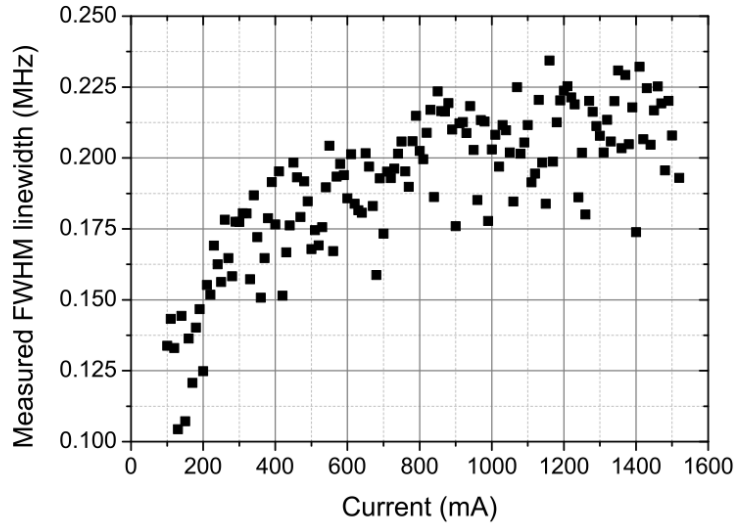


Figure 4. Measured linewidth from 100 mA to 1.5A.

In the linewidth measurements, the devices under test were mounted on AlN submounts and copper heat sinks in a similar manner as in the LIV-measurements. The copper heat sink was water cooled and the temperature was kept at 15°C. The emission linewidth was determined at increasing bias currents by fitting (in the least-squares sense) a Lorentzian lineshape function to the spectra recorded by the electrical spectrum analyzer (ESA) with a frequency resolution of 8.7 kHz. The spectra were averaged over 100 sweeps.

The linewidth measurement results (shown in Figure 4) were obtained after burn-in and illustrate that the lasers can maintain an emission linewidth below 250 kHz over the whole linear operation regime of the LI characteristics.

4.3 Burn-in and reliability tests

Burn-in tests were performed to investigate the early-life behavior of the devices. From the manufacturing batch laser that exhibited unwanted kinks were selected for lifetime tests. Some of the lasers that did not have the best characteristics were attached to an AlN-submount and a copper heat sink and were driven with a 1500 mA bias current for 2000 hours at a 20°C heat sink temperature. Figure 5 illustrates the LI-curve before and after the burn-in test for one of the tested components. It is shown that the threshold current decreases and the mode-hop-free operating range increases after the burn-in. The likely reason for the threshold current decrease is the annealing of some defects. The increased mode-hop-free range could be caused by better alignment of the burn-in-shifted gain spectrum with the grating resonance. It could also be due to reduced defect density, since this leads to reduced temperature increase with current and, consequently, pushes the mode-hop to a higher current.

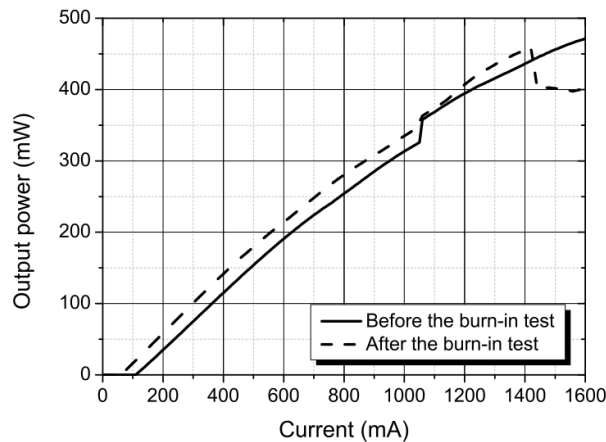


Figure 5. LI-graph showing before burn-in and after burn-in device performance. Burn-in conditions were 2000h, 1.5A and 20°C.

5. CONCLUSION

Manuscript demonstrates the suitability of the GaInNAs Quantum well as a gain material for high power single mode laser operating at 1180 nm. Prepared 1180 nm high power DBR laser diode reach up to 0.5W output power at room temperature and show non-degraded performance over 2000h of operation at high output power.

6. REFERENCES

- [1] V. Korpijärvi, T. Leinonen, J. Puustinen, A. Härkönen, and M. D. Guina, "11 W single gain-chip dilute nitride disk laser emitting around 1180 nm," *Optics express* 18, 25633-25641 (2010).
- [2] M. Kondow, T. Kitatani, S. Nakatsuka, M. C. Larson, K. Nakahara, Y. Yazawa, M. Okai, and K. Uomi, "GaInNAs: a novel material for long-wavelength semiconductor lasers," *Selected Topics in Quantum Electronics* 3, 719-730 (1997).
- [3] A. Jechow, R. Menzel, K. Paschke, and G. Erbert, "Blue-green light generation using high brilliance edge emitting diode lasers," *Laser & Photonics Reviews* 4, 633-655 (2010).
- [4] W. McGee, R. Williams, M. Ashwin, T. Jones, E. Clarke, J. Zhang, and S. Tomić, "Structure, morphology, and optical properties of $\text{Ga}_x\text{In}_{1-x}\text{N}_{0.05}\text{As}_{0.95}$ quantum wells: Influence of the growth mechanism," *Physical Review B* 76, 085309 (2007).
- [5] V.-M. Korpijärvi, A. Aho, P. Laukkanen, A. Tukiainen, A. Laakso, M. Tuominen, and M. Guina, "Study of nitrogen incorporation into GaInNAs: The role of growth temperature in molecular beam epitaxy," *J. Appl. Phys.* 112, 023504 (2012)
- [6] A. Aho, V. -. Korpijärvi, A. Tukiainen, J. Puustinen, and M. Guina, "Incorporation model of N into GaInNAs alloys grown by radio-frequency plasma-assisted molecular beam epitaxy," *J. Appl. Phys.* 116, 213101 (2014).
- [7] M. Hugues, B. Damilano, J. Chauveau, J. Duboz, and J. Massies, "Blue-shift mechanisms in annealed (Ga, In)(N, As)/Ga As quantum wells," *Physical Review B* 75, 045313 (2007).
- [8] K. Paschke, F. Bugge, G. Blume, D. Feise, W. John, S. Knigge, M. Matalla, H. Wenzel, and G. Erbert, "Watt-level continuous-wave diode lasers at 1180 nm with InGaAs quantum wells," *Proc.SPIE* 8965, 896509-896509-7 (2014).
- [9] T. K. Sharma, M. Zorn, F. Bugge, R. Hulsewede, G. Erbert, and M. Weyers, "High-power highly strained InGaAs quantum-well lasers operating at 1.2 μm ," *Photonics Technology Letters* 14, 887-889 (2002).
- [10] J. Viheriälä, J. Tommila, T. Leinonen, M. Dumitrescu, L. Toikkanen, T. Niemi and M. Pessa. "Applications of UV-nanoimprint soft stamps in fabrication of single-frequency diode lasers," *Microelectronic Engineering*, 86(3), 321-324 (2009).
- [11] R. Hui and M. O'Sullivan, "Fiber optic measurement techniques", Academic Press, (2009).
- [12] P. Gallion, F. Mendieta, and R. Leconte, "Single-frequency laser phase noise limitation in single-mode optical-fiber coherent-detection systems with correlated fields" *Journal of the Optical Society of America* 9, 1167-1170, (1982).